

Two-magnon damping in thin films in case of canted magnetization: Theory versus experimentJ. Lindner,^{*} I. Barsukov, C. Raeder,[†] C. Hassel, O. Posth, and R. Meckenstock*Fachbereich Physik and Center for Nanointegration (CeNIDE), AG Farle, Universität Duisburg–Essen, Lotharstr. 1, 47048 Duisburg, Germany*

P. Landeros

Departamento de Física, Universidad Técnica Federico Santa María, Avenida España 1680, Valparaíso, Chile

D. L. Mills

Department of Physics and Astronomy, University of California, Irvine, California 92697, USA

(Received 19 May 2009; revised manuscript received 17 September 2009; published 18 December 2009)

We present results for ferromagnetic resonance measurements in ultrathin magnetic films. Our aim is to investigate quantitatively the damping of spin motions where different sources of damping are present. We investigate a polycrystalline 10-nm-thick Co film grown on GaAs using microwave frequencies between 4 and 24 GHz and different orientations of the static magnetic field. We discuss the role of Gilbert and two-magnon dampings (activated by defects in the film) within the theoretical framework presented some years ago by Arias and Mills [Phys. Rev. B **60**, 7395 (1999)] and its extension to the case in which the magnetization is tipped out of the film plane [P. Landeros, R. E. Arias, and D. L. Mills, Phys. Rev. B **77**, 214405 (2008)]. It is found that linewidth vs. field angle data are well reproduced by the theory for several frequencies and we obtain information about fundamental parameters as well as the role of defects in the dynamical response of the prototype Co system.

DOI: [10.1103/PhysRevB.80.224421](https://doi.org/10.1103/PhysRevB.80.224421)

PACS number(s): 76.60.Es, 75.70.Ak, 75.40.Gb, 76.50.+g

I. INTRODUCTION

The most popular ansatz for the magnetic relaxation in metallic ferromagnetic films is given by the Landau-Lifshitz-Gilbert phenomenology.¹ It was demonstrated, however, that besides intrinsic Gilbert damping, extrinsic mechanisms such as the two-magnon process that describes the defect-mediated scattering of the uniform precession mode into nonuniform ones may strongly alter the overall relaxation or play even a major role.^{2–9} A key feature of the dispersion relation $\omega(k_{\parallel})$ for a thin magnetic film for which spin-wave propagation is confined to the film plane is that when the propagation angle $\varphi_{\vec{k}_{\parallel}}$ defined as the angle between \vec{k}_{\parallel} and the projection of the saturation magnetization M_s into the sample plane is less than the critical value $\varphi_{\text{crit}} = \sin^{-1}\{[H_0/(H_0 + M_{\text{eff}})]^{1/2}\}$ ($M_{\text{eff}} = H_u + 4\pi M_s$, H_u : uniaxial out-of-plane anisotropy field), then the initial slope of the dispersion relation is negative; the minimum spin-wave frequency is at a finite wave vector. Subsequently, for each direction wherein $\varphi_{k_{\parallel}} < \varphi_{\text{crit}}$, there is a mode of finite wave vector degenerate in frequency with the ferromagnetic resonance (FMR) mode. These modes are responsible for two-magnon damping in ultrathin films.^{10–13}

The frequency dependence of the two-magnon scattering has been discussed theoretically for the case that the magnetic field is applied parallel to the film plane^{10–13} and later the description was extended to the case where the magnetization is tipped out of the plane.¹⁴ There, the complete functional dependence of the two-magnon contribution and the out-of-plane angle θ_M of the magnetization vector measured with respect to the film plane was derived. While two-magnon scattering is active for values of $\theta_M < \pi/4$, it shuts off for angles $\theta_M > \pi/4$. This limit is obtained for external

field angles closer to the film normal, depending on the frequency. Without the theoretical description given in Ref. 14, Heinrich and co-workers already addressed the problem of the exact dependence of two-magnon scattering on θ_M in the region $\theta_M < \pi/4$.² They found for Pd-capped Fe/GaAs(001) thin films that the angular dependent deviation between the observed from the expected intrinsic linewidth can be indeed accounted for by two-magnon scattering (see Fig. 5.21 in Ref. 2). Their conclusion was based on the dependence of the critical angle φ_{crit} on the out-of-plane angle θ_M of the magnetization. The result suggested that the scattering matrix of the two-magnon process depends only weakly on θ_M . However, no quantitative comparison to theoretical calculations including a complete two-magnon scattering formalism was performed and the measurements were restricted to a single microwave frequency.

In the present paper, we discuss data for three frequencies which when analyzed quantitatively allow us to make a direct comparison between experiment and the analytic formulas derived in Ref. 14. This is done for thin, polycrystalline Co films grown on GaAs(001). As we shall demonstrate below, the experimental data are accounted for nicely by the theory.

The theoretical papers mentioned so far proposed that random defects located on the film surface or at the interface between the film and the substrate activate the two-magnon mechanism. We note, however, that this assumption can be readily dropped and replaced by a description of defects of known geometry. This raises the possibility that through the tailoring of defect arrays, one may control the nature of the spin damping in ultrathin films through design of defect arrays. The theory in Refs. 10–14 can be extended straightforwardly to explore such possibilities. The analysis presented in the present paper may be viewed as a first step in this

direction, in that we demonstrate that one may achieve a fully quantitative account of the dependence of the two-magnon damping on the direction of the magnetization.

This paper is organized as follows. In Sec. II, we describe the sample preparation, whereas in Sec. III, we briefly resume the theoretical description of two-magnon scattering in case of canted thin-film magnetization. In Sec. IV, we present the experimental results, while Sec. V contains the discussion of comparing theory and experiment.

II. EXPERIMENTAL DETAILS

The polycrystalline Co films are deposited at room temperature by means of electron-beam evaporation in a high-vacuum chamber with a base pressure in the 10^{-9} mbar range on top of 4×4 mm² GaAs(100) substrates. A 10 nm carbon layer has been used to protect the films against oxidation: a procedure already been used in earlier works by us.¹⁵ Standard θ - 2θ x-ray diffraction (XRD) and scanning electron microscopy (SEM) revealed that these films are polycrystalline and have a strong texture along the film normal. While θ - 2θ XRD does not allow to distinguish between fcc[111] and hcp[0001] texture,¹⁶ it is well established in literature that hcp is the stable phase for thin films grown at room temperature.^{16,17} This is also reflected by the fact that the substrate plays almost no role for room-temperature growth of polycrystalline Co with hcp stacking [see, e.g.,¹⁸ where polycrystalline hcp-Co films were grown on Si(001) or glass substrates]. We, thus, presume that our films consist of hcp crystals, but finally mention that the exact knowledge of the stacking sequence of the films does not influence the results to be discussed in the following. The FMR experiments were performed at ambient temperature. Fixed frequencies of 4.06, 9.8, and 23.82 GHz were used, while sweeping the field H_0 up to 17 kG. The external field direction was varied in a plane defined by the film normal and a direction in the film plane (out-of-plane angular dependence). Measurements with varying field direction *within* the film plane revealed no dependence of the FMR signal, i.e., the film behaves isotropic within the plane. The resonance signals were found to be Lorentzian-like at all frequencies. The inset of Fig. 1(b) exemplary shows the signal detected at a microwave frequency of 9.8 GHz for an external field applied in the film plane (resonance at smaller field values) as well as for an external field normal to the film plane. The experimental linewidth was obtained by taking the field difference between the inflection points of the derivative of the Lorentzian (peak-to-peak linewidth). To obtain the saturation magnetization M_s of the film, superconducting quantum interference device (SQUID) magnetometry measurements were additionally performed, revealing $4\pi M_s = 16\,980$ G. Within the experimental error of 5%, resulting mainly from the uncertainty of the sample volume determination, this value is close to the one expected for Co bulk ($4\pi M_s = 17\,600$ G).

III. THEORETICAL BACKGROUND

The FMR frequency is given by^{10,14,19}

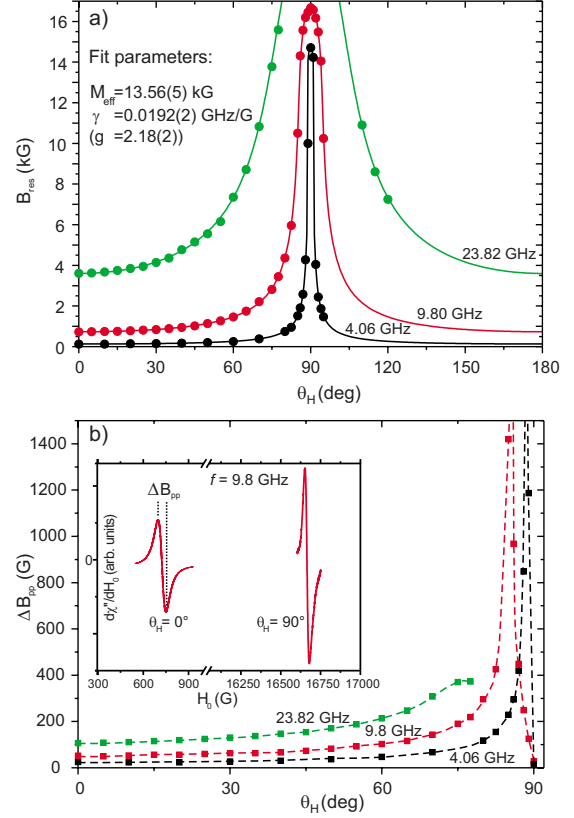


FIG. 1. (Color online) (a) Angular dependence of the resonance field for the frequencies of 4.06, 9.8, and 23.82 GHz. The dots are the experimental data, whereas the lines are fits obtained from Eq. (2) with the parameters mentioned in the text. (b) shows the angular dependence of the FMR linewidth. Note that the x axis is only half of the one shown in (a). Dashed line is a guide to the eyes. Inset shows the spectra detected at 9.8 GHz (X band) for $\theta_H = 0^\circ$ (external field in-plane) and $\theta_H = 90^\circ$ (external field normal to plane).

$$f_{\text{FMR}} = \frac{\gamma}{2\pi} \sqrt{H_X H_Y}, \quad (1)$$

where

$$H_X \equiv H_0 \cos(\theta_H - \theta_M) - M_{\text{eff}} \sin^2(\theta_M),$$

$$H_Y \equiv H_0 \cos(\theta_H - \theta_M) + M_{\text{eff}} \cos(2\theta_M).$$

Here, $\gamma = g\mu_B/\hbar$ is the gyromagnetic ratio given by the g factor. H_0 is the strength of the static magnetic field applied at an angle θ_H with respect to the film plane, θ_M is the (equilibrium) angle of the tipped magnetization with the plane, and $M_{\text{eff}} = H_u + 4\pi M_s$ is the effective magnetization, with M_s the saturation magnetization and H_u the uniaxial out-of-plane anisotropy field; in our theory, the sign convention is such that when $H_u > 0$, the normal to the film surfaces is a hard axis. In Refs. 10, 11, and 14, attention was directed toward very thin films, wherein surface anisotropy was suggested as the dominant contribution to the matrix element which activated two-magnon scattering. The analysis presented by Azevedo and co-workers⁴ provides convincing evidence that this can be so in films with thickness in the 1 nm range. As we

shall see, the thicker films here show no evidence of surface anisotropy, as discussed below. However, surface and interface roughness as well as defects in the volume of the film occurring on short length scales which result in random fluctuations of the direction of the uniaxial anisotropy field H_u can activate two-magnon scattering in a manner very similar to the variations in surface anisotropy considered in the references just cited. The structure of the analysis is the same as in the earlier case for this very similar activation mechanism. We thus in the following assume that H_u is nonuniform throughout the film and it is this nonuniformity which activates two-magnon processes.

Upon writing the equation in the form given above, one assumes that *no* in-plane anisotropy is present. This is consistent with the experimental observation of the absence of any resonance field variation when changing the external field direction within the film plane and is a direct consequence of the polycrystalline nature of our sample.

From the frequency relation, we can write the resonance field as function of the polar out-of-plane angle θ_H as

$$B_{\text{res}} = \frac{1}{2 \cos(\theta_H - \theta_M)} \left[\sqrt{uM_{\text{eff}}^2 + \left(\frac{4\pi f}{\gamma}\right)^2} - vM_{\text{eff}} \right]. \quad (2)$$

Here, $u \equiv \cos^4 \theta_M$ and $v \equiv 1 - 3 \sin^2 \theta_M$ were introduced.

The equilibrium angle of the magnetization can be deduced from minimizing the free energy F of the system which in our case takes the simple form

$$F = -M_s H_0 \cos(\theta_H - \theta_M) + \left(\frac{M_{\text{eff}} M_s}{2}\right) \sin^2 \theta_M. \quad (3)$$

The different sources of damping are reflected by the FMR peak-to-peak linewidth. We use the Arias-Mills formulation^{10,11,14} in which the peak-to-peak linewidth reads

$$\Delta B_{pp} = \Delta B^{(G)} + \Delta B^{(2)}. \quad (4)$$

Here, the first term corresponds to the standard Gilbert damping, which is proportional to the microwave frequency f and is given by

$$\Delta B^{(G)} = \frac{2}{\sqrt{3}} \frac{2\pi f G}{\gamma^2 M_s \Xi}, \quad (5)$$

where we have defined the dragging function

$$\Xi \equiv \cos(\theta_H - \theta_M) - \frac{3H_X + H_Y}{H_Y(H_X + H_Y)} H_0 \sin^2(\theta_H - \theta_M). \quad (6)$$

A deviation of the external field angle θ_H from the equilibrium angle of the magnetization θ_M will lead to an enhanced Gilbert contribution. This effect is called field dragging and is a consequence of magnetic anisotropy fields acting on the magnetization vector. One should note that for either in-plane or out-of-plane external field H_0 , the equilibrium direction of the magnetization will become aligned parallel to H_0 , provided H_0 reaches a critical value (so-called aligned resonance mode, see Ref. 20 for details). Consequently, $\theta_H - \theta_M = 0$ and, in these two cases, no field dragging is present ($\Xi = 1$) so that the linewidth resulting solely from Gilbert damp-

ing found with an external field applied in the film plane is expected to be equal to the case of out-of-plane alignment of H_0 . The dragging function Ξ has its origin in the factor of $df_{\text{FMR}}(\theta_H, \theta_M)/dH_0|_{\theta_H} = \partial f_{\text{FMR}}(\theta_H, \theta_M)/\partial H_0 + (\partial f_{\text{FMR}}/\partial \theta_M)(\partial \theta_M/\partial H_0)$ which appears in the denominator of the expression for the linewidth (see, for instance, the discussion in Ref. 14). In this paper, the term proportional to $\partial f_{\text{FMR}}/\partial \theta_M$ was overlooked. The second term is the contribution of the surface-defect-induced two-magnon scattering mechanism and can be written as (see Eq. 60 in Ref. 14)

$$\Delta B^{(2)} = \frac{2}{\sqrt{3}} \Gamma(H_0, \theta_H) \sin^{-1} \sqrt{\frac{H_X \cos(2\theta_M)}{H_X + M_{\text{eff}} \cos^2 \theta_M}}. \quad (7)$$

In the above expressions, we have multiplied the semihalf linewidth of Refs. 10 and 14 by a factor $2/\sqrt{3}$ in order to obtain the peak-to-peak linewidths determined experimentally. The term $\Gamma(H_0, \theta_H)$ or rather $\Gamma(f)$ is given by¹⁰

$$\Gamma = \frac{8H_u^2 b^2 p / \pi D}{(H_X + H_Y)^2 \Xi} \left\{ \left(\left\langle \frac{c}{a} \right\rangle - 1 \right) H_Y^2 + \left(\left\langle \frac{a}{c} \right\rangle - 1 \right) \times [H_X \cos(2\theta_M) + H_Y \cos^2 \theta_M]^2 + [H_X \cos(2\theta_M) - H_Y \sin^2 \theta_M]^2 \right\}. \quad (8)$$

Here, $D = 2A/M_s$ is the exchange stiffness of the ferromagnetic material. The defects are supposed to cover the fraction p of the film surface and to be rectangular in nature, with lateral dimensions a and c and height (or depth) b if the defect is an island (or a pit) and a and c being randomly distributed.^{10,11} Inspection of Eq. (7) shows that for angles $\theta_M > \pi/4$, the square root becomes negative, which implies that the two-magnon contribution becomes inactive. This observation leads to the conclusion that, whenever the linewidth in the perpendicular geometry ($\theta_H = \theta_M = 90^\circ$) is smaller than in the film plane, two-magnon scattering is likely to contribute to the overall relaxation.

So far, the following analytical formula has been frequently used^{7-9,11,13} to describe the two-magnon relaxation process within thin films:

$$\Delta B_{A-M}^{(2)} = \frac{2}{\sqrt{3}} \Gamma_0 \arcsin \left[\frac{[f^2 + (f_0/2)^2]^{1/2} - f_0/2}{[f^2 + (f_0/2)^2]^{1/2} + f_0/2} \right]^{1/2}, \quad (9)$$

where $f_0 = \gamma M_{\text{eff}} / 2\pi$. It is worth to mention that for the in-plane case ($\theta_H = 0$), the linewidth associated with two-magnon scattering follows very well the above analytical function. Nonetheless, when the applied field (and the magnetization) is tipped out of the plane, the above formula is not appropriate. The reason is that $\Gamma(H_0, \theta_H)$ [see Eqs. (7) and (8)] is a function of H_0 and θ_H and, therefore, is a function of the FMR frequency. In the contrary, Γ_0 in Eq. (9) is a constant.

IV. EXPERIMENTAL RESULTS

We first discuss the angular dependence of the resonance field, followed by the result for the frequency dependence of the linewidth in order to extract information of fundamental

magnetic parameters. These parameters are then used to simulate the general case in which the magnetization is tipped out of the plane by virtue of an applied field. The simulation finally is compared to the experimental data.

A. Resonance field

From the resonance field vs. external field angle θ_H data [see Fig. 1(a)], we can obtain parameters as the gyromagnetic ratio γ and the effective magnetization M_{eff} . We have performed fits of the experimental data to Eq. (2), yielding $M_{\text{eff}}=13.56(5)$ kG and $\gamma=0.0192(2)$ GHz/G [corresponding to a g factor of $g=2.18(2)$]. The parameters perfectly fit the angular dependencies of the FMR resonance field for all three microwave frequencies used. From the values of M_{eff} and $4\pi M_s$ obtained from SQUID magnetometry, one concludes that the difference between $4\pi M_s$ and M_{eff} is given by the uniaxial anisotropy field H_u [i.e., $H_u=-3.4(9)$ kG]. The sign of H_u indicates that it results in an easy axis of magnetization perpendicular to the film plane. The perpendicular character of H_u is a direct result from the Co texture. In what follows, we will use these values whenever we discuss the FMR data.

B. FMR linewidth

1. In-plane and out-of-plane cases

Figure 1(b) shows the (angular-dependent) linewidth data obtained for the Co film at the three frequencies mentioned above. Note that only half of the angular range is shown compared to the resonance field data of Fig. 1(a). The dashed lines are guides to the eyes only. One observes the typical behavior often found for thin-film samples. Starting from in-plane magnetic fields ($\theta_H=0^\circ$), the linewidth slowly increases until it suddenly rises with a steep slope at an angle that decreases with increasing microwave frequency. At higher frequencies, this increase moreover is less pronounced. For fields close to the out-of-plane configuration, the linewidth rapidly decreases again. For exactly out-of-plane fields ($\theta_H=90^\circ$), the linewidth becomes even smaller than for the in-plane geometry. The latter effect can be nicely seen in the inset of Fig. 1(b), where the resonance signal measured at 9.8 GHz with an external field applied in the film plane ($\theta_H=0^\circ$) and normal to the film plane ($\theta_H=90^\circ$) is shown. Note that the much larger resonance field for $\theta_H=90^\circ$ implies that the normal is a hard direction of magnetization. Note that this is a result of the *overall* anisotropy field, given by the sum of the intrinsic field H_u that prefers an easy axis perpendicular to the film plane and the larger shape anisotropy field given by $4\pi M_s$. Before discussing the angular dependence in more detail, in particular the experimental extraction of the pure two-magnon contribution, we focus on the two extreme cases for which the external magnetic field is either aligned in the film plane ($\theta_H=0^\circ$) or normal to it ($\theta_H=90^\circ$).

The frequency-dependent FMR linewidth data for the out-of-plane configuration are represented by the open circles in Fig. 2. In this configuration, the angle of the magnetization with the film plane is bigger than $\pi/4$, so that two-magnon

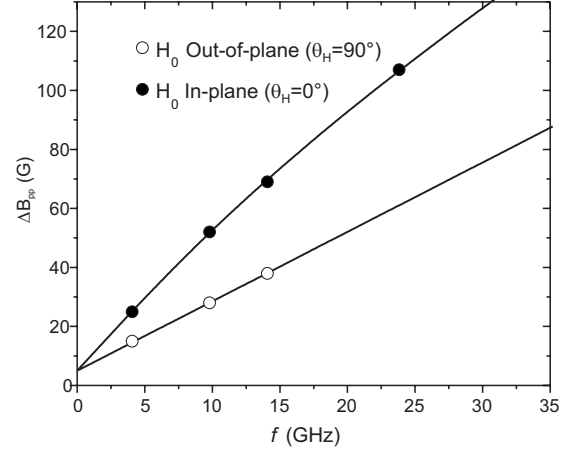


FIG. 2. Peak-to-peak FMR linewidth (ΔB_{pp}) as a function of the frequency for out-of-plane (open circles) and in-plane (filled circles) magnetizations.

effects disappear.^{10,11,14} It follows that the FMR linewidth is given solely by the Gilbert contribution, plus an approximately 5 G offset (frequency-independent inhomogeneous broadening). Thus, we can use Eq. (5) and determine the Gilbert parameter to be $G=0.161(8)$ GHz. Note that the quantity obtained from the fit is actually the value G/M_s which can be converted to G using the value $4\pi M_s \approx 16\,980$ G (from SQUID magnetometry).

For the in-plane case, where the magnetic field and the magnetization lie parallel to the film plane, the two-magnon mechanism is operative and activated by defects in the sample.^{10,11,14} Therefore, the FMR linewidth is composed of Gilbert and two-magnon contributions (filled circles in Fig. 2) and, thus, by fitting the theory to the data, we can obtain information about the parameters related to the extrinsic two-magnon process. In doing this, we have obtained $8H_u^2 b^2 p / \pi D = 118(3)$ G. As stated above, we assume non-uniformity of H_u within our film as likely origin of the two-magnon contribution. We note that although random pits due to surface roughness at the surface of thin films that result in fluctuations of the surface anisotropy field were what the authors of Ref. 10 had in mind when modeling two-magnon processes in such systems, their results can be translated to fluctuations of H_u being a field of uniaxial character just like the surface anisotropy field discussed in Ref. 10. Although the fluctuation of H_u not necessarily has to be present at the surface only, the surface structure of the film may provide a rough estimate of whether the value for $8H_u^2 b^2 p / \pi D$ is plausible. Compared to epitaxial films, which may present roughness on the atomic level, the polycrystalline Co film is assumed to have surface roughness with much larger vertical variations of the film thickness. To further investigate this issue, we have performed atomic force microscopy measurements on a similar Co thin film as the one used for the FMR experiments. For this film, the C-capping layer has been omitted to not have influence on the result. The root-mean-square roughness found was of the order of 0.8 nm. As it describes the standard deviation from a reference plane, the typical height or depth of the surface pits may be assumed to be about 1.6 nm. As we have measured the uniaxial out-of-

plane anisotropy field ($H_u \approx -3.4$ kG), one can calculate the values for b^2p , provided the exchange stiffness parameter is known. Assuming $D \approx 3.4 \times 10^{-9}$ G cm² (Ref. 21) and using the surface roughness above as vertical length scale on which fluctuations in H_u occur, one calculates a defect fraction of about 50%. Although this value should be treated as estimate only, it is a reasonable value.

With the above parameters, we observe very good agreement between the theory and the experiment. We also perform a fit of the data with Eq. (9) from which we extract the parameter $\Gamma_0 = 85(3)$ G, which is simply an average value of $\Gamma(f, \theta_H = 0)$. The other parameter in Eq. (9), that is $f_0 = \gamma M_{\text{eff}} / 2\pi$, has been calculated from the value of M_{eff} obtained from the resonance field curve and using the above-mentioned value of the gyromagnetic ratio γ . With these values, we obtain $f_0 = 41.3(3)$ GHz. We also observe a very good agreement between theory and experiment using Eq. (9), but one has to keep in mind that the approximation of constant Γ does not fulfill the complete angular dependence of two-magnon scattering process and is just valid in the limit of in-plane magnetization and small angles with the film plane. For bigger angles, we use Eqs. (7) and (8).

2. Extraction of the angular-dependent two-magnon contribution

One clearly sees that the two-magnon scattering shuts off at a certain angle depending on the frequency. This effect occurs when the angle of the magnetization achieves the critical value $\theta_M = \pi/4$.

In the following, we discuss how the extraction of the pure two-magnon contribution from the experimental data was performed. As shown by Fig. 1(b), the FMR linewidth shows a steep increase at intermediate angles. This increase is also seen in Fig. 3 where the X-band data (9.8 GHz) again has been plotted without showing the other frequencies. Field dragging, i.e., enhanced Gilbert damping as given by Eq. (5), only accounts for a small portion of the increase. Using the Gilbert parameter obtained from the out-of-plane fit within Eq. (5) results in the dotted green line shown in Fig. 3. Obviously, the Gilbert contribution is too small to explain the huge linewidth increase at intermediate angles.

The behavior of the FMR linewidth of thin films in this region usually is governed not by the intrinsic damping but by inhomogeneous broadening effects. In case that the local resonance field of the film varies as function of the lateral sample position, one will effectively measure a broadened resonance signal. This topic has already been discussed by Chappert *et al.* in Ref. 22 and more recently by Mizukami *et al.*²³ Although our XRD results indicate that the polycrystalline Co film is highly textured, slight lateral variations of the crystallite orientation relative to the substrate normal will intrinsically be present. As we will see, those are responsible for the observed increase of the linewidth in our films. We note that variations due to a thickness dependence of magnetic anisotropies in principle also could be a source of inhomogeneous broadening. Measurements on Co films with different thicknesses of 8–15 nm have, however, revealed that the resonance field does not change within this range. This again reflects that the film under consideration does not

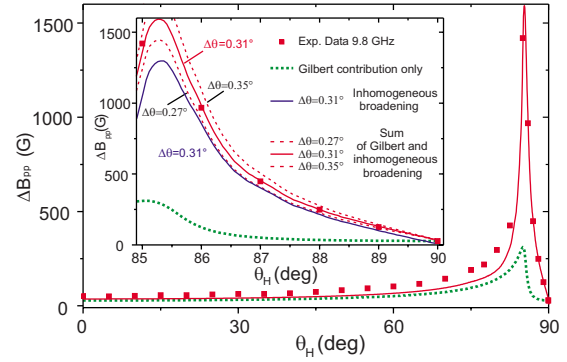


FIG. 3. (Color online) Linewidth as function of the out-of-plane angle of the external field (θ_H) measured at a microwave frequency of 9.8 GHz. Data are plotted as solid squares, the dotted line is a calculation of the angular dependent Gilbert contribution according to Eq. (5), and the solid line represents the sum of Gilbert and angular-dependent inhomogeneous contributions given by Eq. (10) for an angular spread of the easy axes of the Co crystallites with respect to the substrate normal direction of $\Delta\theta_H = 0.31^\circ$. Inset shows a magnification of the region close to the substrate normal for which the two-magnon contribution is inactive (see also Fig. 4). Upper solid line is the sum of Gilbert and inhomogeneous broadening assuming $\Delta\theta_H = 0.31^\circ$, while the two dashed curves assume $\Delta\theta_H = 0.27^\circ$ and $\Delta\theta_H = 0.35^\circ$, respectively. Lower solid line shows the inhomogeneous contribution only assuming $\Delta\theta_H = 0.31^\circ$.

exhibit a significant contribution from surface anisotropy as mentioned earlier.

Inhomogeneous broadening due to an angular spread in the crystallite orientation is given by^{22,23}

$$\Delta B^{\text{inhom}} = \frac{\partial B_{\text{res}}}{\partial \theta_H} \Delta \theta_H. \quad (10)$$

Here, $\Delta\theta_H$ is the angular variation of the normal orientation of the crystallites. The derivative has to be calculated from the angular dependence of the resonance field already shown in Fig. 1(a). One notes that, whenever the resonance field dependence has a steep slope (strong dependence on θ_H), inhomogeneous broadening will be large and this, in fact, in the case for the intermediate angular region for which a large linewidth is observed. For the in-plane ($\theta_H = 0^\circ$) and out-of-plane ($\theta_H = 90^\circ$) cases, however, inhomogeneous broadening is inactive as can be deduced from the vanishing slope of the resonance field dependence for these geometries [see Fig. 1(a)]. Thus, the argumentation used above to extract the Gilbert damping remains valid.

To find the value of the angular spread $\Delta\theta_H$, we have fitted Eq. (10) to our data optimizing the fit for θ_H values close to the out-of-plane direction at $\theta_H = 90^\circ$. The lower θ_H limit of this fitting procedure was chosen to be the external field angle θ_H^{crit} for which the angle of the magnetization θ_M equals $\pi/4$, i.e., for which two-magnon scattering becomes inactive. This ensures that only the inhomogeneous broadening and Gilbert damping contribute within the interval $\theta_H^{\text{crit}} - 90^\circ$. The best fit using Eq. (10) and the plausible value $\Delta\theta_H = 0.31^\circ$ is shown in Fig. 3 by the solid blue line (the inset shows a magnification of the angular region of interest).

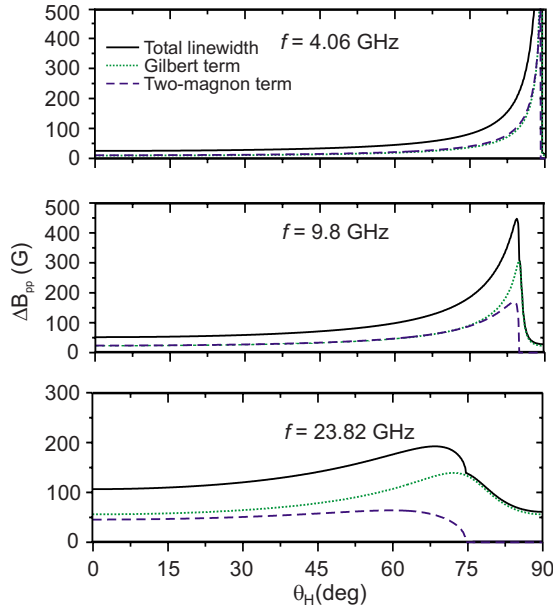


FIG. 4. (Color online) Calculated FMR peak-to-peak linewidth (ΔB_{pp}) as a function of the field angle for different frequencies. We include contributions from two-magnon scattering (dashed lines) and Gilbert damping (dotted lines) and a small offset of 5 G. Solid lines show the sum of all contributions.

The Gilbert contribution (dotted green line) has been added within this fitting procedure, finally yielding the red line as overall contribution. Due to the steep slope of the linewidth dependence in the interval $\theta_H^{\text{crit}} - 90^\circ$, the error of $\Delta\theta_H = 0.31^\circ$ is rather small. The two other curves representing the Gilbert and an inhomogeneous contribution with $\Delta\theta_H = 0.27^\circ$ and $\Delta\theta_H = 0.35^\circ$ (red dashed lines in the inset) indicate that the error is about 5%. The value of $\Delta\theta_H = 0.31^\circ$ was also used to calculate the contributions for the other two experimental frequencies (not shown here). In summary, the procedure described so far enables one to (i) eliminate all other contributions to the experimental overall linewidth except the two-magnon one and—from the in-plane and out-of-plane cases—(ii) to extract the parameters needed for performing the theoretical calculation of the angular-dependent two-magnon contribution (effective anisotropy field M_{eff} that includes the uniaxial out-of-plane anisotropy field and the film magnetization, g factor, and the prefactor of the two-magnon contribution given by $8H_u^2 b^2 p / \pi D$).

C. Theoretical results for arbitrary magnetization directions and comparison to experiment

Now we proceed to calculate theoretically the FMR linewidth in the case where the magnetization is tipped out of the plane. The detailed discussion of the procedure may be found in Ref. 14. In Fig. 4, we show the results for the angular dependence of the FMR linewidth including contributions from standard Gilbert damping as given by Eq. (5) (dotted lines) and two-magnon scattering (dashed lines) plus the small offset mentioned already in the description of the experimental data. For the calculation, we have used the parameters obtained in the previous section and we plotted the

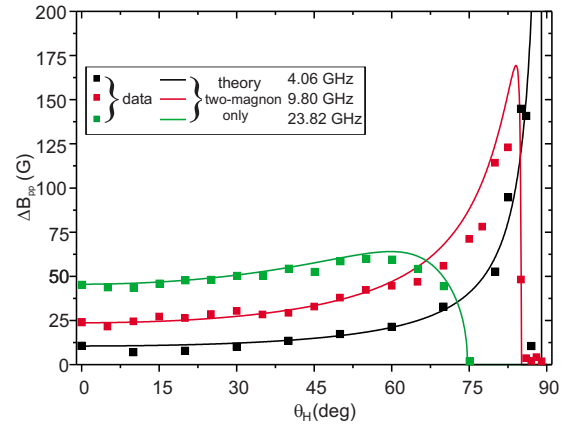


FIG. 5. (Color online) Experimental data (squares) and simulation (solid lines) for the two-magnon contribution only.

result for the frequencies used within our experiments (indicated in the Figure). The solid lines are the sum of all contributions. It becomes evident that the two-magnon scattering is inactive for a given angle which decreases as function of the microwave frequency. Closer inspection shows that the angle is given by the external field angle for which the magnetization encloses an angle of $\pi/4$ with respect to the film plane. As the resonance fields increase as function of the microwave frequency [see Fig. 1(a)], this critical angle of the magnetization decreases with microwave frequency or, in other words, the magnetization vector follows—at larger microwave frequencies—the external field more closely while anisotropy fields become less important.

One further sees that for our system, the Gilbert and two-magnon contributions are almost equal in magnitude. Only at the highest frequency of 23.82 GHz the Gilbert contribution slightly overcomes the two-magnon one, which is a consequence of the fact that Gilbert damping scales linear with frequency while two-magnon scattering saturates for larger frequencies. The angular dependence of two-magnon scattering at higher microwave frequencies is indeed rather constant within a wide-angle range before it shuts off. This behavior is similar to the one discussed by Heinrich for Fe thin films in Ref. 2. However, at low microwave frequencies, the scenario changes and one observes a monotonic increase of the contribution until becoming inactive.

Finally, we directly compare the theoretical simulations to the experimental result. Note that all parameters which are necessary for the theoretical calculations are pinned down from measurements with external field in the film plane and normal to it (see discussion above). No more free parameter is used to model the complete angular dependence. In Fig. 5, we present the calculated angular dependencies of the two-magnon contribution for all three microwave frequencies (solid lines) on top of the experimentally extracted two-magnon data (squares). The figure shows that we find very good agreement between theory and experiment. The shut off at larger external field angles as well as the behavior for smaller angles is reproduced by the experimental result. We clearly find that the behavior strongly depends on the microwave frequency. Not only the shut-off angle, but also the dependence at smaller angles differs as function of f . While

at lower frequencies two-magnon scattering increases when the external field is tipped out of the film plane, it remains almost constant at larger frequencies.

V. CONCLUSION

Using microwave frequencies of 4.06, 9.8, and 23.82 GHz for room-temperature investigations on a prototype Co thin film of polycrystalline nature, we have shown that the theoretical description presented earlier in Ref. 14 is capable of quantitatively describing the effect of canted magnetization on the FMR linewidth in thin magnetic films. Besides, the classic Gilbert damping two-magnon damping may influence and strongly alter the dependence. The results provide a way to predict magnetic damping for arbitrary external field direction for systems for which two-magnon scattering plays an important role. As—in contrast to Gilbert damping—two-

magnon scattering is an extrinsic effect which can, in principle, be influenced by incorporating defects into the film, the result also yields a possibility to controllably tune magnetic damping, since theory is able to predict the size of defects as well as their influence on the overall magnetic relaxation.

ACKNOWLEDGMENTS

We gratefully acknowledge support of the first author (J.L.) by the Alexander von Humboldt Foundation through the Feodor Lynen Program. The work was further partially supported by the Deutsche Forschungsgemeinschaft, Project No. Sfb 491, the program “Bicentenario en Ciencia y Tecnología” PBCT under Project No. PSD-031, FONDECYT Project No. 11080246 (Chile). The research of D.L.M. has been supported by the U.S. Army through Contract No. CS000128.

*juergen.lindner@uni-due.de

†Present address: Deutsches Zentrum für Luft- und Raumfahrt e.V., Institut für Technische Thermodynamik–Solarforschung, Linder Höhe, Geb. 3e, 51147 Köln, Germany.

¹T. L. Gilbert, *IEEE Trans. Magn.* **40**, 3443 (2004); Ph.D. thesis, Illinois Institute of Technology, 1956.

²B. Heinrich, *Spin Relaxation in Magnetic Metallic Layers and Multilayers, Ultrathin Magnetic Structures*, edited by J. A. C. Bland and B. Heinrich, *Fundamentals of Nanomagnetism Vol. III*, (Springer, Berlin, 2005).

³M. J. Hurben and C. E. Patton, *J. Appl. Phys.* **83**, 4344 (1998).

⁴A. Azevedo, A. B. Oliveira, F. M. de Aguiar, and S. M. Rezende, *Phys. Rev. B* **62**, 5331 (2000).

⁵R. D. McMichael and P. Krivosik, *IEEE Trans. Magn.* **40**, 2 (2004).

⁶B. J. Kuanr, R. E. Camley, and Z. Celinski, *J. Appl. Phys.* **95**, 6610 (2004).

⁷J. Lindner, K. Lenz, E. Kosubek, K. Baberschke, D. Spoddig, R. Meckenstock, J. Pelzl, Z. Frait, and D. L. Mills, *Phys. Rev. B* **68**, 060102(R) (2003).

⁸K. Lenz, H. Wende, W. Kuch, K. Baberschke, K. Nagy, and A. Jánossy, *Phys. Rev. B* **73**, 144424 (2006).

⁹Kh. Zakeri, J. Lindner, I. Barsukov, R. Meckenstock, M. Farle, U. von Hörsten, H. Wende, W. Keune, J. Rucker, S. S. Kalari-ckal, K. Lenz, W. Kuch, K. Baberschke, and Z. Frait, *Phys. Rev. B* **76**, 104416 (2007).

¹⁰R. Arias and D. L. Mills, *Phys. Rev. B* **60**, 7395 (1999).

¹¹R. Arias and D. L. Mills, *J. Appl. Phys.* **87**, 5455 (2000).

¹²D. L. Mills and S. M. Rezende, in *Spin Dynamics in Confined Magnetic Structures II*, edited by B. Hillebrands and K. Ounadjela (Springer, New York, 2003).

¹³D. L. Mills and R. Arias, *Physica B* **384**, 147 (2006).

¹⁴P. Landeros, R. E. Arias, and D. L. Mills, *Phys. Rev. B* **77**, 214405 (2008).

¹⁵M. Brands, O. Posth, and G. Dumpich, *Superlattices Microstruct.* **37**, 380 (2005).

¹⁶K. H. Lee, H. S. Lee, J. Y. Lee, T. W. Kim, K. H. Yoo, and Y. S. Yoon, *Mater. Res. Bull.* **39**, 1369 (2004).

¹⁷H. Wieldraaijer, J. T. Kohlhepp, P. LeClair, K. Ha, and W. J. M. de Jonge, *Phys. Rev. B* **67**, 224430 (2003).

¹⁸A. Kharmouche, J. Ben Youssef, A. Layadi, and S.-M. Chérif, *J. Appl. Phys.* **101**, 113910 (2007).

¹⁹H. Suhl, *Phys. Rev.* **97**, 555 (1955).

²⁰S. V. Vonsovski, *Ferromagnetic Resonance* (Pergamon, Oxford, 1960).

²¹X. Liu, M. M. Steiner, R. Sooryakumar, G. A. Prinz, R. F. C. Farrow, and G. Harp, *Phys. Rev. B* **53**, 12166 (1996).

²²C. Chappert, K. L. Dang, P. Beauvillain, H. Hurdequint, and D. Renard, *Phys. Rev. B* **34**, 3192 (1986).

²³S. Mizukami, Y. Ando, and T. Miyazaki, *Jpn. J. Appl. Phys.* **40**, 580 (2001).